Wind and Structures, *Vol. 27, No. 6 (2018) 399-416*
DOI: https://doi.org/10.12989/was.2018.27.6.399

Case study of random vibration analysis of train-bridge systems subjected to wind loads

Siyu Zhu[1], Yongle Li[*2], Koffi Togbenou[2], Chuanjin Yu[2] and Tianyu Xiang[3]

[1]College of Environment and Civil Engineering, Chengdu University of Technology, 610059, Chengdu, Sichuan, P.R. China
[2]Department of Bridge Engineering, Southwest Jiaotong University, 610031, Chengdu, Sichuan, P.R. China
[3]Department of Civil and Structural Engineering, The Xihua University, 610031, Chengdu, Sichuan, P.R. China

(Received January 6, 2018, Revised April 30, 2018, Accepted May 4, 2018)

Abstract. In order to reveal the independent relationship between track irregularity and wind loads, the stochastic characteristics of train-bridge coupling systems subjected to wind loads were investigated by the multi-sample calculation. The vehicle was selected as 23 degrees of freedom dynamical model, and the bridge was described by three-dimensional finite element model. It was assumed that the wind loads were random processes with strong spatial correlation, while the track irregularities were stationary random ones. As a case study, a high-speed train running on a cable-stayed bridge subjected to wind loads was studied. The effect of rail irregularities was deemed to be independent of the effect of wind excitations on the coupling system in the same wind circumstance for the same project, leading to the conclusion that the effect of wind loads and moving vehicle could be calculated separately. The variance results of the stochastic responses of vehicle-bridge coupling system under the action of wind loads and rail irregularities together were equivalent to the sum of the variance of the responses induced by each excitation. Therefore, when one of the input excitations is different, only the effect of changed loads needs to be assessed. Moreover, the new calculated results were combined with the effect of unchanged loads to present the stochastic response of coupling system subjected to the different excitations, reducing the cost of computations. The stochastic characteristics, the CFD (cumulative distribution function) of the coupling system with different wind velocities, vehicle speed, and vehicle marshalling were studied likewise.

Keywords: train-bridge systems; stochastic characteristic; independent relationship; wind loads; track irregularity

1. Introduction

The rapid development of high-speed railway technology has resulted in modern railway system with various bridge structures to ensure the comfort of passenger and, more importantly, the safety and stability of running trains (Madshus *et al*. 2000, Raghunathan *et al*. 2002). Bridge are undeniably an imperative element in railway structure, given that bridges account for about 80.5% of the length of the Beijing-Shanghai high-speed railway in China. Modern high-speed trains are light in weight, and this has remarkably increased the probability for train-bridge coupling system to be affected by wind loads. Thus, the dynamic analysis of train-bridge subjected to wind loads has received increasing attention and awareness (Cai *et al*. 2015, Cheli *et al.* 2010, Kwon *et al*. 2008, Petrini and Bontempi 2011). Li *et al*. (2005) proposed the wind-vehicle-bridge coupling vibration model in time domain. His model was based on the solid contact of vehicle-bridge, the effect of wind on the bridge and vehicle, the temporal correlation during transportation of train on the bridge, and the interaction between wind and bridge. Xu *et al*. (2004) built the dynamic analysis framework of cable-stayed bridge-vehicle subjected to lateral wind. The stable and unstable aerodynamic forces were simulated in time domain and applied on the vehicle model. The effect of vehicle running speed and correlation of aerodynamic space on bridge was investigated.

The pioneering studies have established a solid foundation for further research. However, when the railway vehicles are passing through the bridges, the interactions between the two subsystems display strong stochastic characteristics. The theory of random vibration should be used to calculate the dynamic responses of vehicle-bridge coupling system. Aua *et al.* (2002) simulated a ten degrees of freedom vehicle model and a two-dimensional bridge structure to calculate the stochastic vibration of vehicle-bridge subjected to rail-irregularities. Lu *et al.* (2009) proposed an effective method to solve the random response of non-stationary coupling system. Majka *et al.* (2009) investigated the effect of bridge skewers and random track irregularities on dynamic response of train running through bridge and evaluated bridge response depending on the calculated results. Prof. Lin's research team (Lin *et al.* 2004, Jiahao 1992, Lin *et al*. 1994) gave a significant contribution to the stochastic response of vehicle-bridge coupling system. Based on the theory of pseudo excitation method, multi-dimensional pseudo excitation method was derived. Lombaert *et al*. (2012) solved the interaction of vehicle-bridge in frequency domain and directly calculated the connection between vehicle and bridge by Fourier transform.

The external excitations, e.g., earthquake or wind load,

*Corresponding author, Professor
E-mail: lele@swjtu.edu.cn

http://www.techno-press.com/journals/was&subpage=7 ISSN: 1226-6116 (Print), 1598-6225 (Online)

does not only increase the vibration of vehicles and bridges (ElGawady and Sha'lan 2011, Prenninger *et al.* 1990), but also it strongly make the vehicle-bridge coupling system vibrate more randomly. PEM (the pseudo excitation method) has been proved to be valid for the time-dependent system (Lin *et al*. 2011) and is widely used in wind-induced vibration of structures (Caprani 2014, Xu *et al*. 1999). Zhang *et al.* (2010, 2011) calculated random vibration of train-bridge subjected to earthquake. It applied to transform the lateral seismic waves and rail irregularities into the vehicle-bridge coupling system and proved the independent relationship between track irregularities and earthquake. Xu *et al.* (1999) focused on the slender structure subjected to wind excitation with or without control devices and validated an advanced method to solve it. Xu *et al.* (1997) and Duan *et al.* (2011) also used the PEM to investigate wind-induced flutter-buffet analysis of Hong Kong Tsing-Ma suspension bridge. However, the spatial correlation of wind loads is extremely strong in the turbulent wind field. The wind speed and direction of several points are different for the same windward side. Consequently, random wind loads are multi-point coherent excitation. In general, wind processes at several locations are necessary to simulate the wind field of long-span bridge (Deodatis 1996, Shinozuka, 1971) and the frequency of wind excitation should contain the vibration frequency of bridge and vehicle. When computation cost is of interest, PEM may not offer high efficiency and is not suitable to calculate the stochastic response of vehicle-bridge subjected to wind loads. The effect of seismic loads is independent from the effect of rail irregularities on the coupling system. However, the independent relationship between wind load and rail irregularities is not determined.

In this paper, the stochastic response of vehicle-bridge coupling system subjected to wind loads is calculated by Monte Carlo method. 500 samples of wind excitation and rail irregularities are simulated; every simulated sample for each excitation is independent. Since all the calculated samples for every case have the same time step and the same length of calculating time, the time histories of results also possess the same time step and length of time. Nerveless, every time-step result for the calculated cases could be calculated to gain the corresponding standard deviation. Based on the 500 time histories of the dynamic responses, the time histories of standard deviation of coupling system could be calculated. Firstly, since the independent characteristic between wind excitation and rail irregularities is not proved, three cases of the random responses were calculated. Case 1 and Case 2 investigate the response of the coupling system under rail irregularities only and wind loads only respectively, while Case 3 includes both of excitations for the computation of the coupling system response. Investigation on the dependency between the wind excitation and the excitation caused by track irregularities could remarkably reduce the computation cost, without sacrificing accuracy by decreasing the amount of computation and the time of computation. When one of the two excitations (i.e., wind loads and rail irregularities) changes, only the effect of the varied excitation parameter needs to be studied, then the simple superposition approach is applied to calculate the final result. Secondly, the effect of vehicle speed, wind speed, and marshalling of vehicle are studied. Finally, based on the random responses of coupling system, the CFD (cumulative distribution function) is calculated to evaluate the vibration of the coupling system.

2 Model of vehicle-bridge coupling system subjected to wind loads

The analysis framework of vehicle-bridge coupling system is composed of vehicle model and bridge structure. The vehicle with four axles and two bogies is selected in this paper with 23 degrees of freedom (DOF). The wind loads are regarded as the external load inputs to the coupling system.

2.1 Vehicle model

The single-organization railway vehicle includes several components, e.g., one vehicle body, two bogies and four wheel-sets, which are assumed as rigid body and connected by spring and damper, as shown in Fig. 1. The whole vehicle is considered as a mass-spring-damper dynamic model. The spring provides the flexibility of the vehicle system, and the dampers simulate the energy-dissipating devices such as rubber pads and shock absorbers. Vehicle is assumed to be moving at a constant speed along a straight line without considering the derailment phenomena. Therefore, the DOF along the traveling direction for every rigid body can be neglected. Consequently, there are 5 DOFs for every train body and bogie, i.e., lateral movement, floating, rolling, yawing, and nodding. Since the rail track vibration is ignored and the wheel-set is in contact with the rail track, there are only 2 independent DOFs for a wheel-set: lateral movement and yawing. All the parameters are based on the existing analysis model (Xu *et al*. 1997). As a result, a four-axle vehicle has 23 DOFs which scarify the dynamic characteristics of real railway vehicle. To verify the established vehicle model in this paper, the frequency and vibration shape are compared with the data in the published literatures, as shown in Table 1 (Wu *et al.* 2001). The results showed that the established model has a great agreement with the existing model (Li *et al*. 2010).

The equations of the vehicle system with wind loads can be expressed as follows

$$\mathbf{M}_v\ddot{\mathbf{Y}}_v + \mathbf{C}_v\dot{\mathbf{Y}}_v + \mathbf{K}_v\mathbf{Y}_v = F_{bv} + F_{stv} + F_{buv} \tag{1}$$

Where $\ddot{\mathbf{Y}}_\text{v}$, $\dot{\mathbf{Y}}_\text{v}$ and $\mathbf{Y}_\text{v}$ are the acceleration, velocity, and displacement vector of the vehicle, respectively; and $\mathbf{M}_\text{v}$、$\mathbf{C}_\text{v}$ and $\mathbf{K}_\text{v}$ are the mass matrix, the damping matrix, and the stiffness matrix of vehicles, respectively. F_{bv} is the vector of wheel-rail interaction forces at the wheel–rail contact points. F_{stv} and F_{buv} are the static loads and buffeting loads for vehicle.

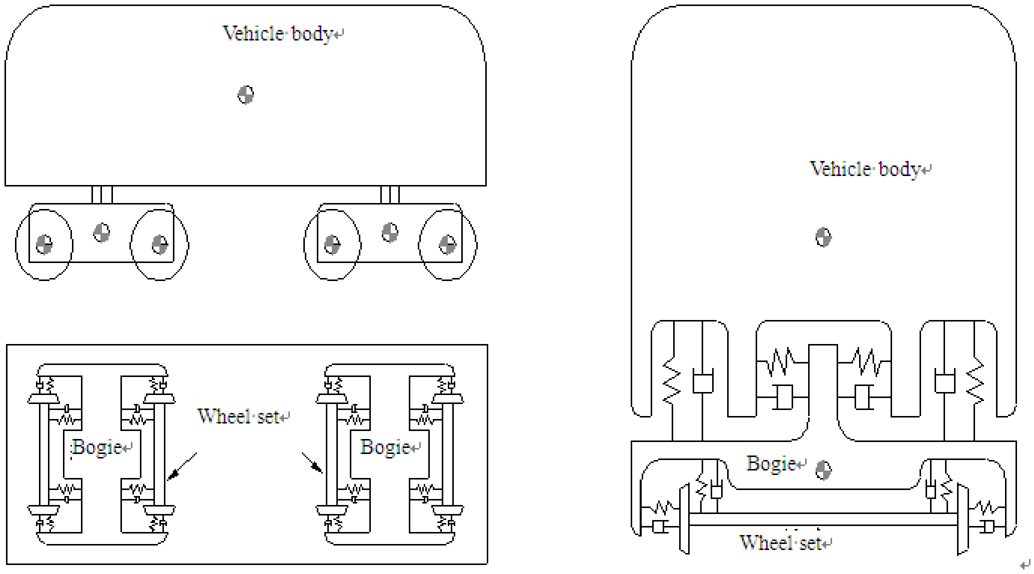

Fig. 1 Vehicle dynamic model

Table 1 The dynamic charateristic of vehicle model

Order	Tranditional model (Wu *et al*. 2001) (Hz)	Established model (Hz)	Vibration shape
1	0.0000	0.0000	Rigid-body Movement
2	0.0000	0.0000	Rigid-body Movement
3	0.7229	0.7228	Vehicle body Floating
4	0.8914	0.8913	Vehicle body Rolling
5	0.8949	0.8980	Vehicle body Nodding
6	1.2446	1.2446	Bogie Yawing
7	1.2488	1.2488	Bogie Yawing
8	1.3940	1.3939	Bogie Lateral Movement
9	1.6695	1.6694	Bogie Lateral Movement
10	4.9194	4.9194	Bogie Floating
11	4.9262	4.9262	Bogie Floating
12	6.3019	6.3018	Bogie Nodding
13	6.3019	6.3018	Bogie Nodding
14	7.0384	7.0383	Bogie Rolling
15	7.0577	7.0577	Bogie Rolling
16	11.8190	11.8190	Wheel-sets Yawing
17	11.8290	11.8190	Wheel-sets Yawing
18	12.4520	12.4520	Wheel-sets Lateral Movement
19	12.4530	12.4530	Wheel-sets Lateral Movement
20	25.8180	25.8180	Wheel-sets Yawing
21	25.8180	25.8180	Wheel-sets Yawing
22	37.5180	37.5170	Wheel-sets Yawing
23	37.5180	37.5170	Wheel-sets Yawing

2.2 Bridge model

The FE model of a long-span cable-stayed bridge can be established by ANSYS software. The girders, towers, and piers are regarded as 3D-beam elements and the cables as 3D-link elements. The secondary dead loads of the bridge are selected as additional mass elements. The equation of motion for the bridge is shown below

$$\mathbf{M}_b\ddot{\mathbf{Y}}_b+\mathbf{C}_b\dot{\mathbf{Y}}_b+\mathbf{K}_b\mathbf{Y}_b=F_{vb}+F_{stb}+F_{bub}+F_{seb} \quad (2)$$

Where $\ddot{\mathbf{Y}}_b$, $\dot{\mathbf{Y}}_b$ and $\mathbf{Y}_b$ are the acceleration, velocity, and displacement vector of the bridge, respectively; and $\mathbf{M}_b$, $\mathbf{C}_b$ and $\mathbf{K}_b$ are the mass matrix, the damping matrix, and the stiffness matrix of the bridge, respectively. The lumped mass matrix is used in the study and the structural damping is assumed to be Rayleigh damping. F_{vb} is the vector of the wheel-rail interaction forces. F_{st}, F_{bu} and F_{se} are static loads, buffeting loads and self-excited loads of bridge, respectively.

2.3 Rail irregularities

When the bridge and vehicle model is establishing, the wheel-rail contact point is defined in both of the models. The rail irregularities are simulated, then the time histories is input into every contact point. Rail irregularities are the main influence factor to the vehicle vibration (Gullers *et al*. 2008). In general, rail irregularities are approximately treated as a stationary stochastic process. In this paper, rail irregularities are simulated by the following equation

$$u_r(t)=\sqrt{2}\sum_{k=1}^{N}\sqrt{2S(\omega_k)\Delta\omega}\cos(\omega_k t+\phi_k) \quad (3)$$

where $x(t)=-\sum_{i=1}^{p}a_i x(t-i\Delta t)+u(t)$ is the spectrum of rail irregularities. $\omega_k=\omega_{min}+(N-\frac{1}{2})\Delta\omega,(k=1,2,\ldots,N)$ is the discrete frequency for the spectrum, $\Delta\omega=(\omega_{max}-\omega_{min})/N$ is the frequency increment, ω_{max} and ω_{min} are the maximum and minimum frequency, respectively. ϕ_k is an independent random phase angle uniformly distributed between 0 and 2π with a density of $1/(2\pi)$.

The bridge is a high-speed railway whose vehicle design velocity is up to 350 km/h and thus German rail irregularity spectra for high speed railway are adopted as follows

$$S_y(\Omega)=\frac{A_v\cdot\Omega_c^2}{(\Omega^2+\Omega_r^2)(\Omega^2+\Omega_c^2)}(m^2/(rad/m)) \quad (4a)$$

$$S_z(\Omega)=\frac{A_a\cdot\Omega_c^2}{(\Omega^2+\Omega_r^2)(\Omega^2+\Omega_c^2)}(m^2/(rad/m)) \quad (4b)$$

$$S_\theta(\Omega)=\frac{A_v\cdot(0.75)^{-2}\cdot\Omega_c^2\cdot\Omega^2}{(\Omega^2+\Omega_r^2)(\Omega^2+\Omega_c^2)(\Omega^2+\Omega_s^2)}(m^2/(rad/m)) \quad (4c)$$

where Ω is the space frequency; A_a (=2.19×10^{-7} m/rad) A_v (=4.032×10^{-7} m/rad) are the roughness parameters; Ω_c (=0.8246 rad/m), Ω_r (=0.0206 rad/m), Ω_s (=0.4380 rad/m) are the break frequencies.

2.4 Wind excitation

Based on the theory of wind-induced vibration, the wind loads include three parts: static wind loads induced by the mean part of the wind flow, the buffeting loads resulted by the random wind fluctuation and the self-excited loads reflecting the aero-elastic interactions between wind and deck (Jones and Scanlan 2001, Yongle Li *et al*. 2005).

2.4.1 Wind loads for bridge

Static wind loads

Static wind loads are induced by the mean value of wind flow. For line-like structure, static wind loads are usually expressed by three components: drag, lift and moment as follows

$$F_D=\frac{1}{2}\rho U^2 C_D(\alpha_0)D \quad (5a)$$

$$F_L=\frac{1}{2}\rho U^2 C_L(\alpha_0)B \quad (5b)$$

$$F_M=\frac{1}{2}\rho U^2 C_M(\alpha_0)B^2 \quad (5c)$$

where ρ is the air density ; U is the mean wind speed ; $C_D(\alpha_0),C_L(\alpha_0),C_M(\alpha_0)$ are the drag, lift and moment coefficients, respectively ; B is the width of body along the mean wind flow and H is the cross-wind projected area (per unit length) normal to the main stream direction.

In general, the aerodynamic parameters are functions of the angle of attack, which could be obtained by the section model test in the wind tunnel. When vehicles are moving on a specific segment of the deck, the aerodynamic effect of the vehicles should be taken into account in the determination of the aerodynamic coefficients of the segment of deck. The aerodynamic loads on the vehicles are also affected by the geometrical shape of deck section. The wind tunnel experiment is performed to acquire the aerodynamic coefficients of vehicle-bridge coupling system which is considering the aerodynamic influence between bridge and vehicle. When the aerodynamic coefficients of bridge deck are tested, the bridge deck model set on the testing equipment and the vehicle mode just hang above and noncontact the bridge deck. It leads that the testing aerodynamic coefficients could not be affected by the gravity of vehicle model and the aerodynamic influences of vehicle shape is considering. Whereas, when the aerodynamic coefficients of vehicle are tested, the vehicle model set on the testing equipment and bridge deck model hang down and no touch the vehicle model.

Buffeting loads

Buffeting loads are induced by stochastic wind fluctuations. According to the quasi-steady theory, buffeting loads on deck and on pylon can be expressed as follows

$$\begin{aligned} D_{bu}(x,t) &= \frac{1}{2}\rho U^2 B\left[2C_D(\alpha_0)\frac{u(x,t)}{U}\gamma_1 + C_D'(\alpha_0)\frac{w(x,t)}{U}\gamma_2\right] \\ L_{bu}(x,t) &= -\frac{1}{2}\rho U^2 B\left\{2C_L(\alpha_0)\frac{u(x,t)}{U}\gamma_3 + [C_L'(\alpha_0)+C_D(\alpha_0)]\frac{w(x,t)}{U}\gamma_4\right\} \\ M_{bu}(x,t) &= \frac{1}{2}\rho U^2 B^2\left[2C_M(\alpha_0)\frac{u(x,t)}{U}\gamma_5 + C_M'(\alpha_0)\frac{w(x,t)}{U}\gamma_6\right] \end{aligned} \quad (6)$$

D_{bu}, L_{bu}, M_{bu} are drag, lift and moment buffeting loads; α_0 is the angle between bridge deck and wind flow; C_D', C_L', C_M' are the slopes of C_D, C_L, C_M ; $u(x,t)$ is the wind velocity fluctuation in mean wind flow direction; $w(x,t)$ is the wind velocity fluctuation in the vertical direction for deck or in the span wise direction for pylons. $\gamma_1 \sim \gamma_6$ are the aerodynamic admittance functions.

For the flat streamlined box girder section, aerodynamic admittance functions of bridge deck could be approximated by the simplified flat Tablet aerodynamic admittance function. For the passivated cross-section, the aerodynamic admittance functions could be approximated as 1.0, which means that the effect of aerodynamic admittance functions is ignored.

Self-excited loads

To consider the test accuracy of all the parameters, the self-excited loads can be expressed as follows

$$D_{se} = \frac{1}{2}\rho U^2 B\left[KP_1^*\frac{\dot{P}}{U} + KP_2^*\frac{B\dot{\alpha}}{U} + K^2P_3^*\alpha\right] \quad (7a)$$

$$L_{se} = \frac{1}{2}\rho U^2 B\left[KH_1^*\frac{\dot{h}}{U} + KH_2^*\frac{B\dot{\alpha}}{U} + K^2H_3^*\alpha + K^2H_4^*\frac{h}{B}\right] \quad (7b)$$

$$M_{se} = \frac{1}{2}\rho U^2 B^2\left[KA_1^*\frac{\dot{h}}{U} + KA_2^*\frac{B\dot{\alpha}}{U} + K^2A_3^*\alpha + K^2A_4^*\frac{h}{B}\right] \quad (7c)$$

where P_i^*, H_i^*, A_i^* （i=1,4） is flutter derivative of bridge deck; $K = \frac{B\omega}{U}$ is the reduced frequency. ω is excitation frequency of wind loads.

P_i^*, H_i^*, A_i^* are function in frequency-domain which cannot be applied in time-domain analysis. Lin (Li and Lin, 1995, Lin and Li 1993) thought self-excited loads are produced by linear mechanism which could be presented by the convolution of impulse response function. The flutter derivative of vertical and torsional bridge deck could be gained by section model test. The lateral derivative just needs the first three functions which can be expressed as follow

$$P_1^*(k) = -2C_D/K, P_2^*(k) = C_D'/K, P_3^*(k) = C_D'/K^2 \quad (8)$$

2.4.2 Wind loads for vehicle

The wind loads for vehicle are similar to the wind loads for bridge, including static wind loads, buffeting loads and self-excited loads. For long railway vehicle, its lateral aerodynamic coefficient approximately follows the cosine rule. The static loads and buffeting loads of vehicle are similar to the function of bridge deck. When train is running on the bridge in longitudinal direction, the aerodynamic coefficient is constant in the whole process. The vertical and lateral wind velocity fluctuations of vehicle are determined by the vehicle location in every time step. The wind speed is same between vehicle model and bridge model at the same location when vehicle is moving, the fluctuating wind speed for vehicle should be the time histories at different simulation point. Since the width of vehicle is narrow and the cross section is passive, the aerodynamic coupling effect is weak. Thus, the self-excited loads for vehicle are ignored.

2.5 The equation of motion of vehicle-bridge coupling system subjected to wind loads

The bridge is established using the finite element method, the track is assumed to be attached firmly to it and the wheels are assumed to remain in close contact with the track. The interaction between vehicle and bridge is presented by their own movement. Thus, bridge and vehicle could be regarded as two subsystems. The equation of motion of the coupling system subjected to wind loads is expressed in the following form

$$\begin{bmatrix} \mathbf{M}_b & 0 \\ 0 & \mathbf{M}_v \end{bmatrix}\begin{Bmatrix} \ddot{u}_b \\ \ddot{u}_v \end{Bmatrix} + \begin{bmatrix} \mathbf{C}_b & 0 \\ 0 & \mathbf{C}_v \end{bmatrix}\begin{Bmatrix} \dot{u}_b \\ \dot{u}_v \end{Bmatrix} + \begin{bmatrix} \mathbf{K}_b & 0 \\ 0 & \mathbf{K}_v \end{bmatrix}\begin{Bmatrix} u_b \\ u_v \end{Bmatrix} = \begin{Bmatrix} F_{stb} + F_{bub} + F_{seb} + F_{vb} \\ F_{stv} + F_{buv} + F_{bv} \end{Bmatrix} \quad (9)$$

The subscript **b** and **v** indicates respectively the bridge and vehicle. F_{st}, F_{bu} and F_{se} is the static wind loads, buffeting loads and self-excited wind loads, respectively. F_{vb} is the interaction force between vehicle and bridge caused by vehicle. F_{bv} is the interaction force between vehicle and bridge caused by bridge.

3. Case study

3.1 Engineering background

The numerical computations involved a long-span cable-stayed railway bridge. The prototype structure has two towers. The total length of the main bridge is 640 m, with a span arrangement of 60+135+250+135+60 m. The finite element model of structures is necessary to obtain

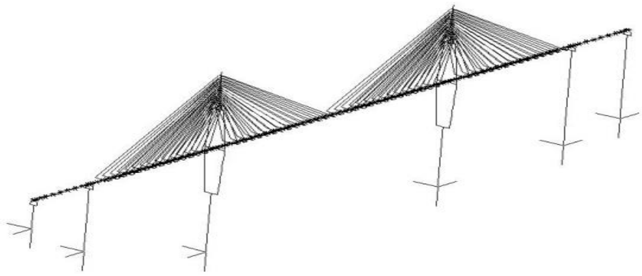

Fig. 2 The element finite model of bridge

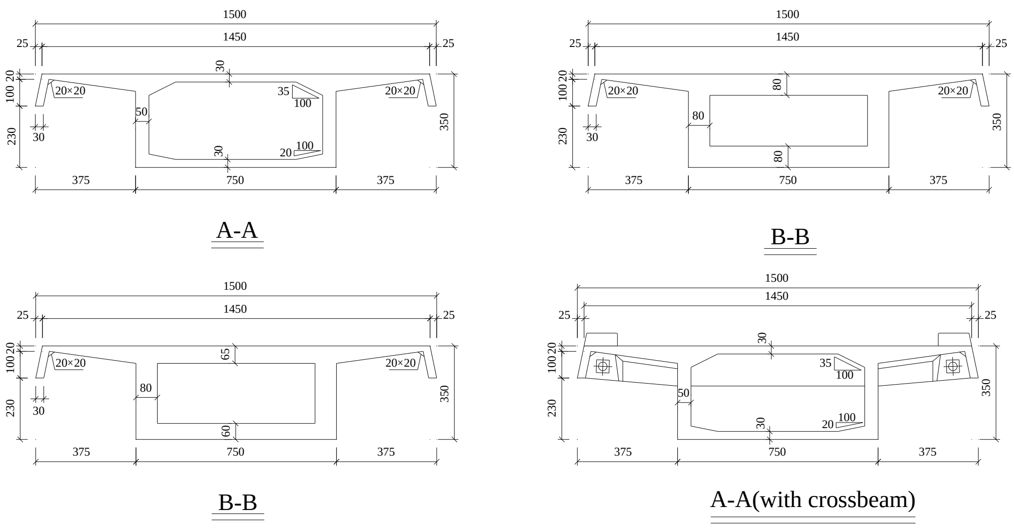

Fig. 3 The cross section of main bridge

Table 2 Structural natural frequencies and model shapes

Order	Natural frequency (Hz)	Mode shape
1	0.2552	Tower lateral symmetric vibration
2	0.2951	Tower lateral asymmetric vibration
3	0.3007	Main girder longitudinal moving
4	0.3701	Tower lateral asymmetric vibration
5	0.3829	Mound longitudinal moving
6	0.4339	1st vertical mode-symmetric
7	0.5393	1st lateral mode-symmetric
8	0.7264	1st vertical mode-asymmetric
9	0.7702	1st lateral mode-asymmetric
10	0.8992	2nd lateral mode-symmetric

these responses which can reflect the dynamic characteristic of structural dynamic responses, as shown in Fig. 2. The bridge cross-section is shown in Fig. 3. The damping radio is 0.02, the height of main girder is 3.5 m and the width of girder is 15 m. There is a diaphragm at every cable anchorage location on the deck. The main towers are made of reinforced concrete structures with the diamond shape. The whole bridge has 56 pairs of cables where the spacing on bridge deck is 8 m and the spacing on tower is 2.2 m.

The girder is made of C60 concrete whose elasticity modulus is 3.6×10^4 Mpa and Poisson radio is 0.2.

C40 and C30 concrete are selected for the bridge towers and the foundation, respectively. The density of all the concretes is 2600 kg/m^3. Imposing initial strain on element is used to simulate the cable force. Besides, the elasticity modulus of cable is 1.95×10^5 Mpa, Poisson radio of cable is 0.2 and the density of cable is 7800 kg/m^3. The dynamic characteristic of bridge is calculated in ANSYS software, and the result is shown in Table 2.

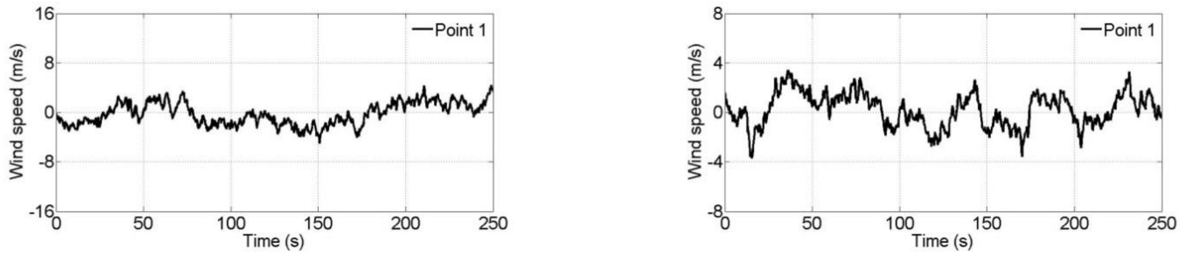

Kaimal Spectrum–Point 1 Panofsky Spectrum–Point 1

Fig. 4 Simulated wind velocities (Point 1)

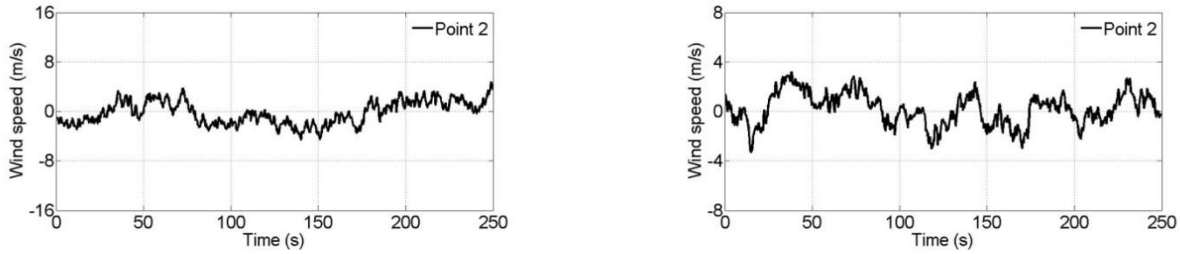

Kaimal Spectrum–Point 2 Panofsky Spectrum–Point 2

Fig. 5 Simulated wind velocities (Point 2)

Table 3 the aerodynamic coefficient of vehicle and bridge of main bridge

Object	C_D	C_L	C_M	C'_D	C'_L	C'_M
Vehicle	0.8616	-0.6930	0.1076	-2.495	4.396	1.680
Bridge	1.4665	-0.0868	0.0502	-0.314	0.690	0.632

3.2 Stochastic wind velocity field

Wind velocity field is one of the most significant excitations of vehicle-bridge coupling system. A hybrid approach of space-time random-field based SRM and proper orthogonal decomposition (POD)-based interpolation is developed for simulating the wind velocity process (Peng *et al*. 2016). According to geographic and geomorphic characteristics of the bridge location, the surface roughness is C type and the influence factor α is 0.22 (*01-2004 J T G T D. Wind-resistant Design Specification for Highway Bridges*, 2004) . The basic wind velocity in bridge location is 27.5 m/s. Since the height between bridge deck and water surface is 111.072 m, K_1 is 1.333 (*01-2004 J T G T D. Wind-resistant Design Specification for Highway Bridges*, 2004) and standard wind speed of bridge deck is estimated as follows

$$U_d = K_1 U_{10} = 1.333 \times 27.5 = 36.7 m/s \tag{4}$$

U_d is mean wind velocity at the height of bridge deck. U_{10} is mean wind velocity at the height of 10 m. K_1 is constant which is checked in reference (*01-2004 J T G T D. Wind-resistant Design Specification for Highway Bridges*, 2004).

Based on the wind tunnel test, the aerodynamic coefficients and the slopes of the bridge and vehicle are estimated and shown in Table 3. According to the wind-resistant design specification, the lateral and vertical spectra are selected as Kaimal and Panofsky spectrum whose expressions are shown as follows

$$\frac{nS(z,n)}{u_*^2} = \frac{200f}{(1+50f)^{\frac{5}{3}}} \tag{11a}$$

$$\frac{nS(z,n)}{u_*^2} = \frac{6f}{(1+4f)^2} \tag{11b}$$

where f is the dimensionless normalized frequency, $f = \frac{nz}{U(z)}$, $U(z)$ is mean wind velocity at the height z; n is frequency in Hz ; u_* is shear velocity of the flow.

The time histories of wind field are simulated to analyze the dynamic responses of vehicle-bridge coupling system subjected to wind loads.

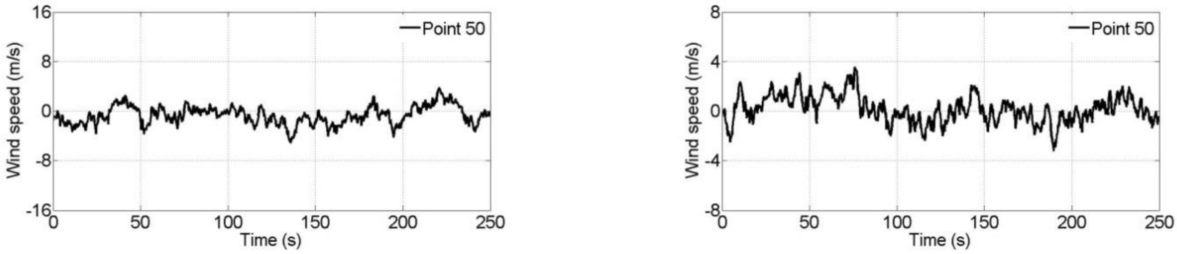

Kaimal Spectrum–Point 50 Panofsky Spectrum–Point 50

Fig. 6 Simulated wind velocities (Point 50)

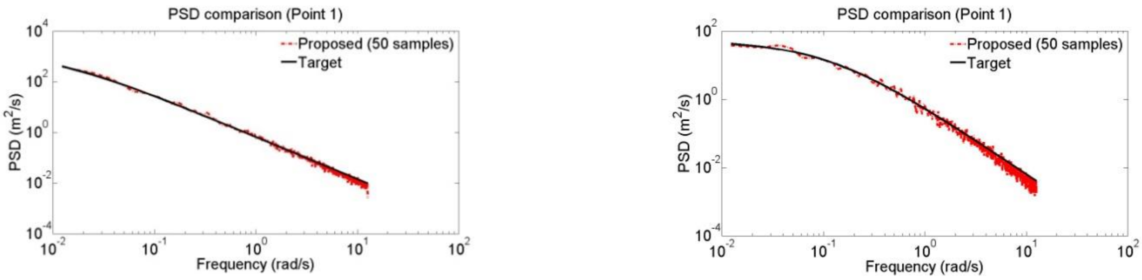

Kaimal Spectrum Panofsky Spectrum

Fig. 7 PSD functions at Point 1

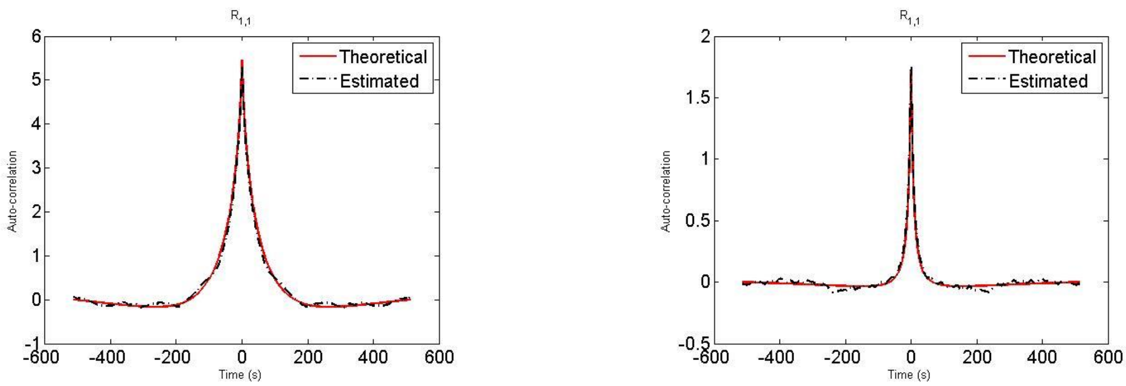

Kaimal Spectrum Panofsky Spectrum

Fig. 8 Auto correlation function at Point 1

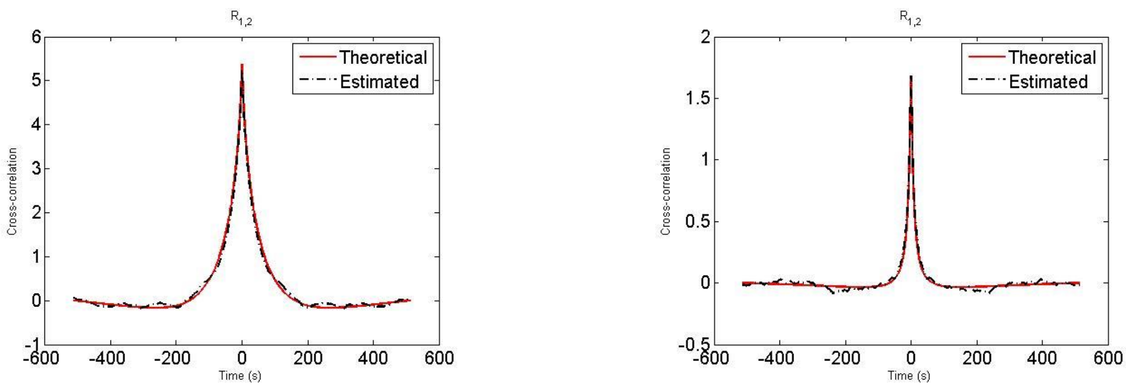

Kaimal Spectrum Panofsky Spectrum

Fig. 9 Comparison of cross correlation functions between Point 1 and Point 2

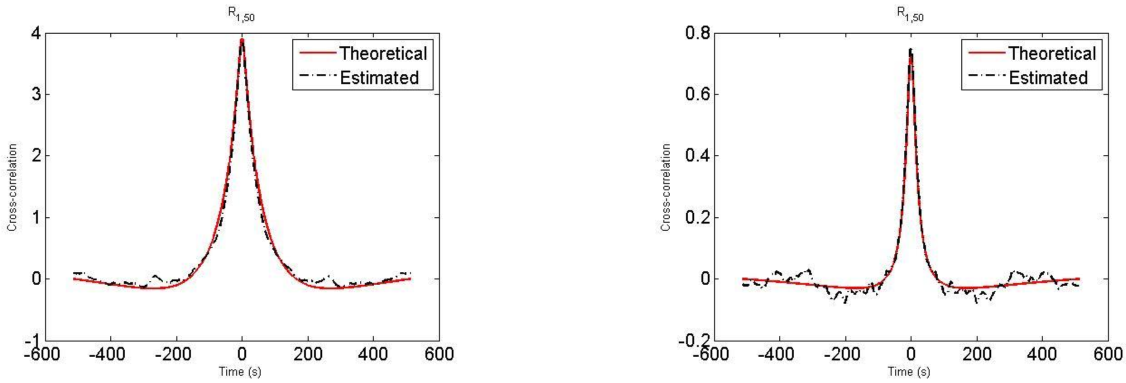

Kaimal Spectrum Panofsky Spectrum

Fig. 10 Comparison of cross correlation functions between Point 1 and Point 50

The simulated wind frequency is 0~2π rad/s. The discrete norm of frequency is 2048. The discrete norm of wave is 1024. The wind speed is 20 m/s. The wind speed time-histories at Point 1, Point 2 and Point 50 are shown in Figs. 4-6.The cross correlation functions and the auto correlation functions among the three points are also calculated as shown in Figs. 7-10. The simulated PSD, auto correlation and cross correlation functions have a great agreement with their corresponding targets.

3.3 The independent relationship between wind loads and rail irregularities

To address the random characteristic of vehicle-bridge coupling system subjected to wind loads, the whole history of single train marshalling running through the bridge is simulated. The parameters for the case study are as follows: vehicle running speed is 250 km/h, the time step is 0.025 s, and the total time steps is 430. The frequency range of rail irregularities is 0.1~3 Hz and that of wind loads is 0~3 Hz, the mean wind velocity is 20 m/s.

The relationship between the effect of wind excitation and rail irregularities on the stochastic response of coupling system is investigated. Therefore, three cases are considered: the wind loads are the only excitations for the coupling system (Case 1) which is showed the Only Wind curve in Figs. 11 and 12, the rail irregularities are the only excitations (Case 2) which is showed the Only Rail curve in Figs. 11 and 12 and the hybrid excitation which combined wind loads and rail irregularities (Case 3). The Case 3 is presented the Original curve in Figs. 11 and 12. The standard deviations of all the cases are shown in Fig 11 and Fig. 12. Besides, Combined curve means the square root of sum of the variance of Case 1 and Case 2 which follows the Eq. (11).

$$\sigma_{w-r} = \sqrt{\sigma_w^2 + \sigma_r^2} \tag{11}$$

σ_{w-r} is the value of the combined curve in Figs. 11 and 12; σ_w is the standard deviation of Case 1 ; σ_r is the standard deviation of Case 2.

As shown in Figs. 11 and 12, the wind loads dominated the standard deviation of bridge responses, the influences of track irregularities on coupling system is relatively small. The Original curves have a great agreement with the Combined curves for all the responses of bridge. However, the contribution of track irregularities is much smaller than the wind loads on standard deviation of bridge responses. So the persuasion of agreement between those two curves is not sufficient to prove the dependency between wind loads and track irregularities. For the standard deviation of vehicle responses, the effect of track irregularities on stochastic responses of vehicle-bridge coupling system subjected to wind loads is significant. The contribution of track irregularities approximately equal to the contribution of wind loads on standard deviation of vehicle. Taking the vertical acceleration of vehicle as an example, the maximum of standard deviation of Case 1 is 0.0648 m/s^2, and Case 2 is 0.0692 m/s^2. Comparing the Original curve with the Combined curve, it is shown that there exist some discrepancies among the responses of vehicle, and the vertical acceleration is most obvious. This is caused by the fact that the influence of track irregularities on system random vibrations is significant. Also, train running speed will correspondingly induce the time-lags between the wheel excitations and wind loads. Besides, the track irregularities play a most important role in vertical acceleration of vehicle among the whole responses. With the increasing the number of calculated samples, the errors between those two curves could be much smaller.

Nevertheless, the vehicle responses also have an essential agreement between the responses under combined wind and wave loads and the results calculated from the simple superposition approach based on the Eq. (11). Therefore, the dependency between the effect of wind loads and the effect of track irregularities on standard deviation of coupling system is proved. The effect of wind loads is independent of the rail irregularities, which would significantly reduce the computation cost.

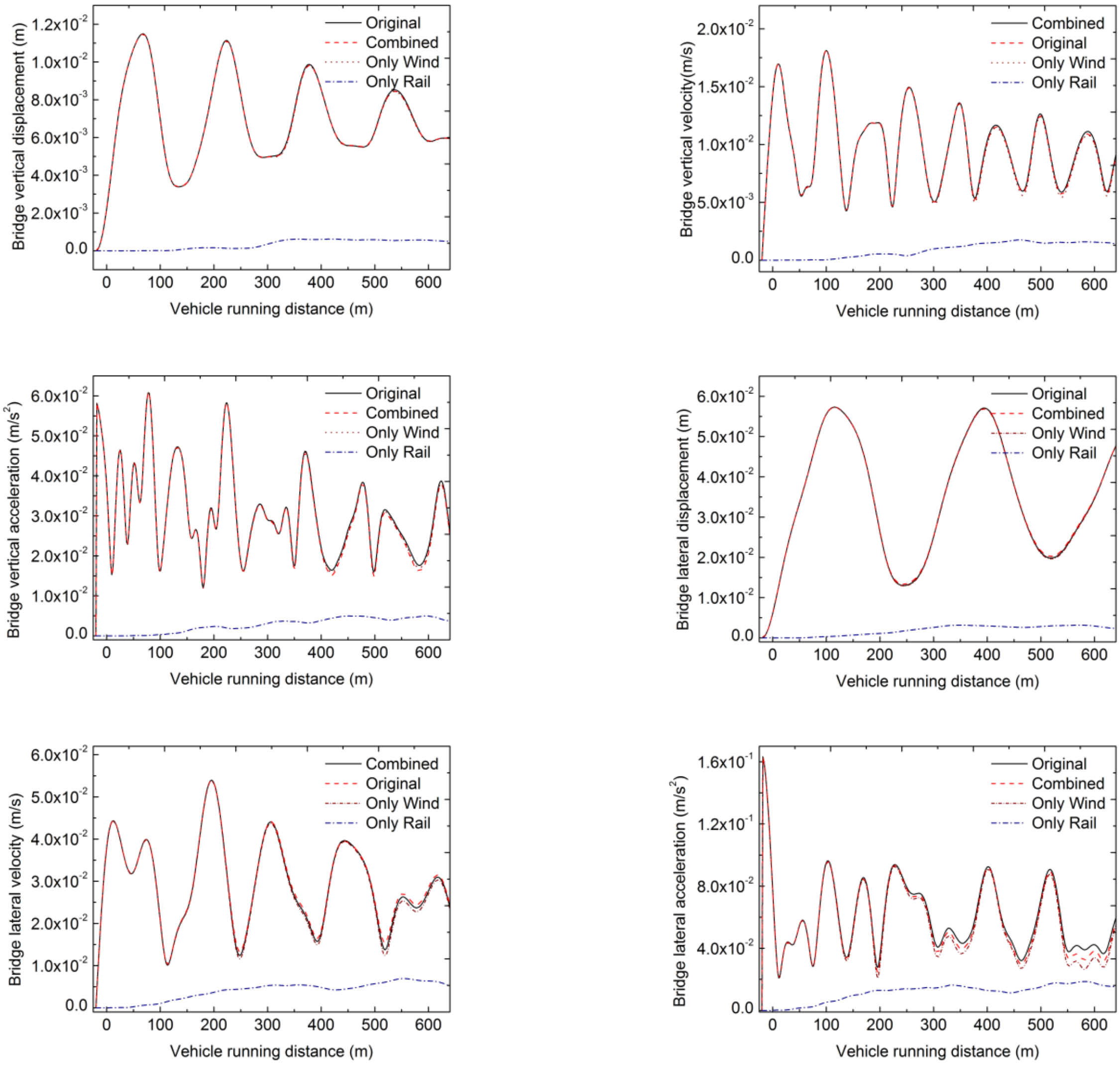

Fig. 11 The standard deviation of bridge responses

3.4 The effect of vehicle running speed on the coupling system subjected to wind loads

The standard deviation of vehicle-bridge coupling system subjected to wind loads at different vehicle running speed is calculated.

Running speed of 200 km/h, 250 km/h, 300 km/h and 350 km/h are selected to study the effect of running speed on the stochastic response. The standard deviation of coupling system is shown in Figs. 13 and 14. As shown in the calculated results (in Figs. 13 and 14), the different vehicle running speed has a significant influence on the vehicle responses. Firstly, taking the maximum of vertical acceleration of vehicle as example, the acceleration reaches the maximum when the vehicle running at the middle of bridge. For the all cases at the different running speed, the maximum for all cases is 0.082 m/s^2; the maximum is 0.121 m/s^2, which is 1.48 times as big as the minimum. Besides, the non-stationarity of vertical responses for vehicle is increasing with the growth of the running speed. Since the wind loads make the vehicle-bridge coupling system have non-stationary characteristics, the stochastic responses of coupling system are more sensitive to the external excitations. Secondly, the CDF (cumulative distribution function) of the bridge and vehicle acceleration for all the cases is presented in Fig. 15. The vertical acceleration of vehicle appears regularity rising with the increasing running speed. But the lateral acceleration reveals the irregular variation. When running speed reaches 300 km/h, the lateral response is much smaller than the other cases. The CDF of other three cases is similar which shows the same variations with the standard deviation in Fig. 14. Finally, since the effect of running speed on the bridge responses is very low, the acceleration responses of bridge have little noticeably change which appear at the running speed 350 km/h in vertical acceleration for system and the 200 km/h in lateral acceleration for bridge. The vertical acceleration of bridge when running speed reaches 350 km/h is obviously different from the other cases. But the difference between 350 km/h and the other cases is decreasing with the increasing

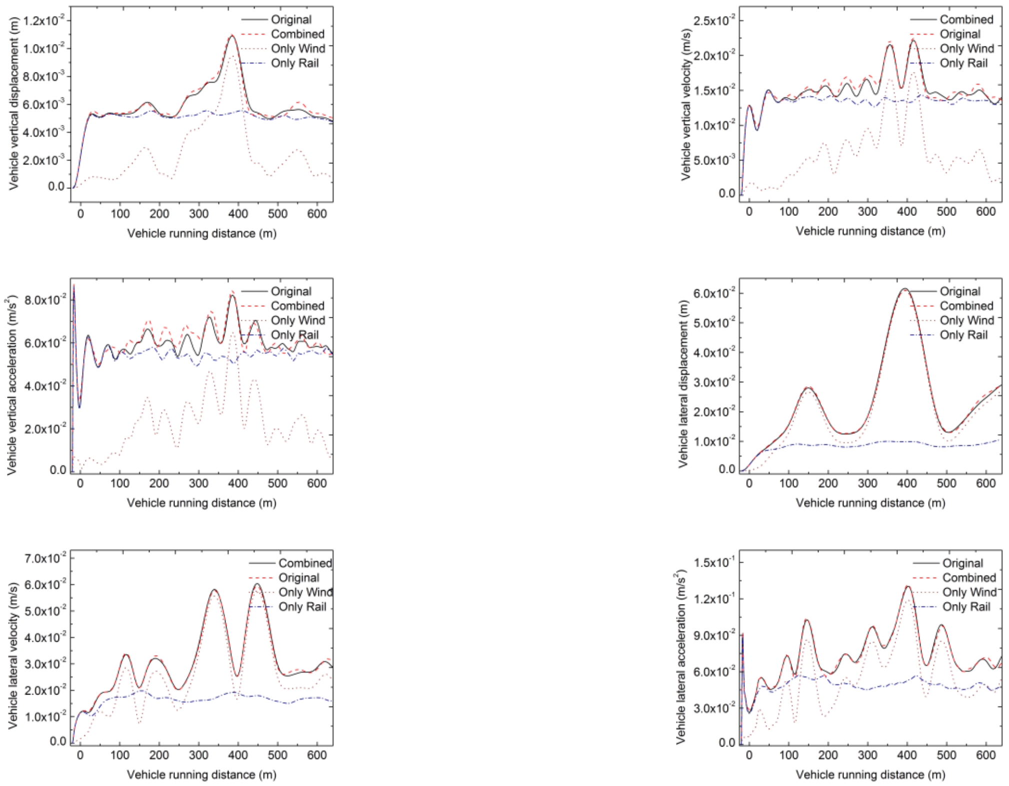

Fig. 12 The standard deviation of vehicle responses

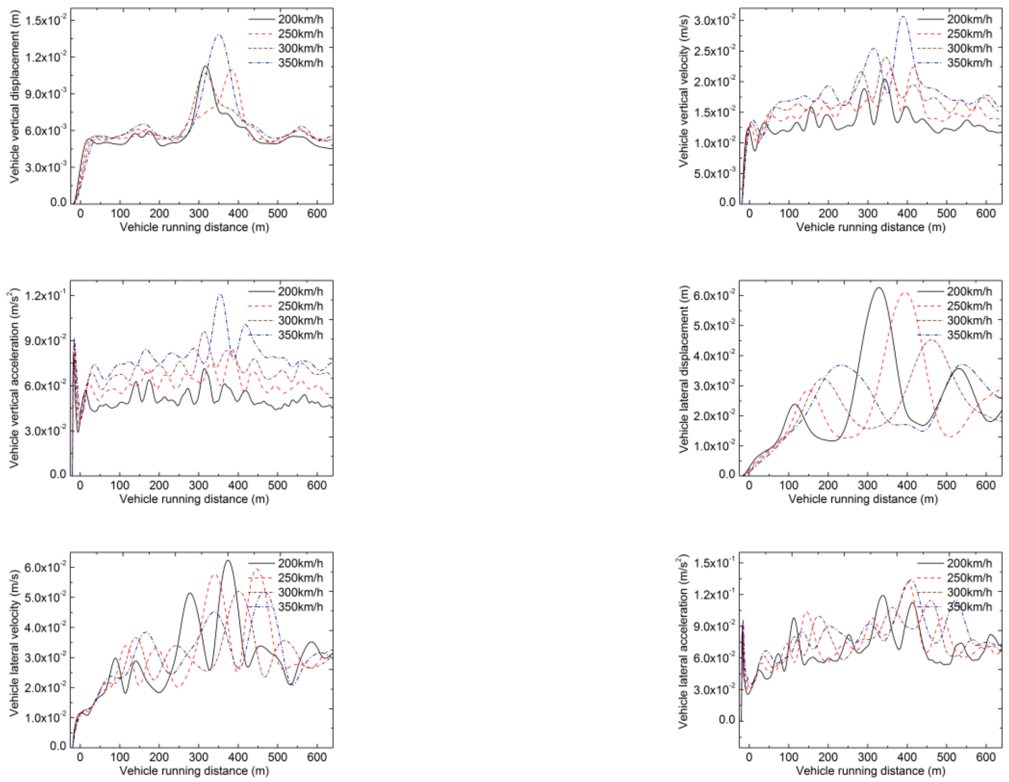

Fig. 13 The standard deviation of vehicle responses with different running speed

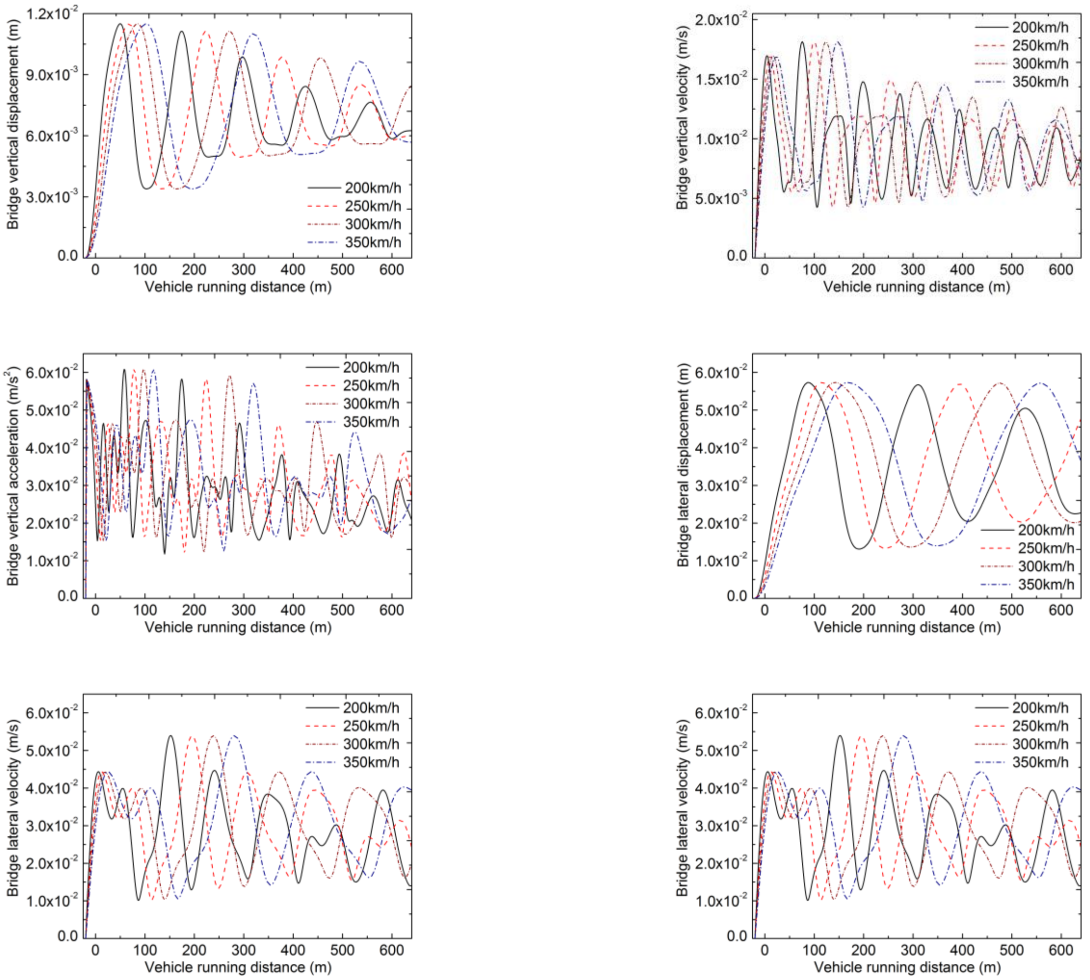

Fig. 14 The standard deviation of bridge responses with different running speed

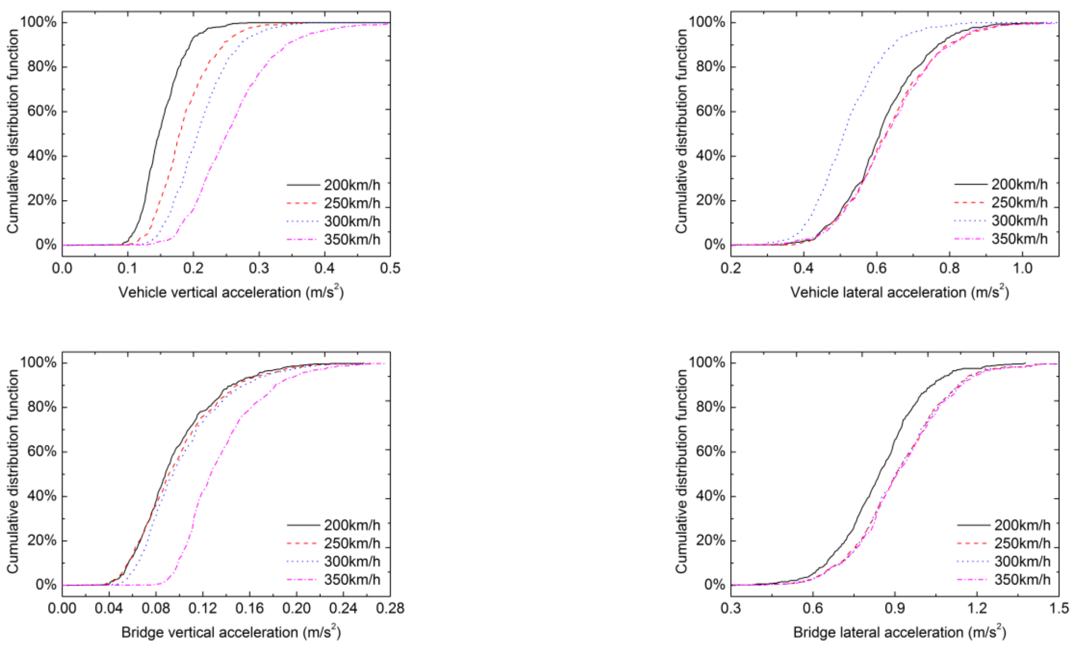

Fig. 15 The CDF of vehicle-bridge coupling system with different running speed

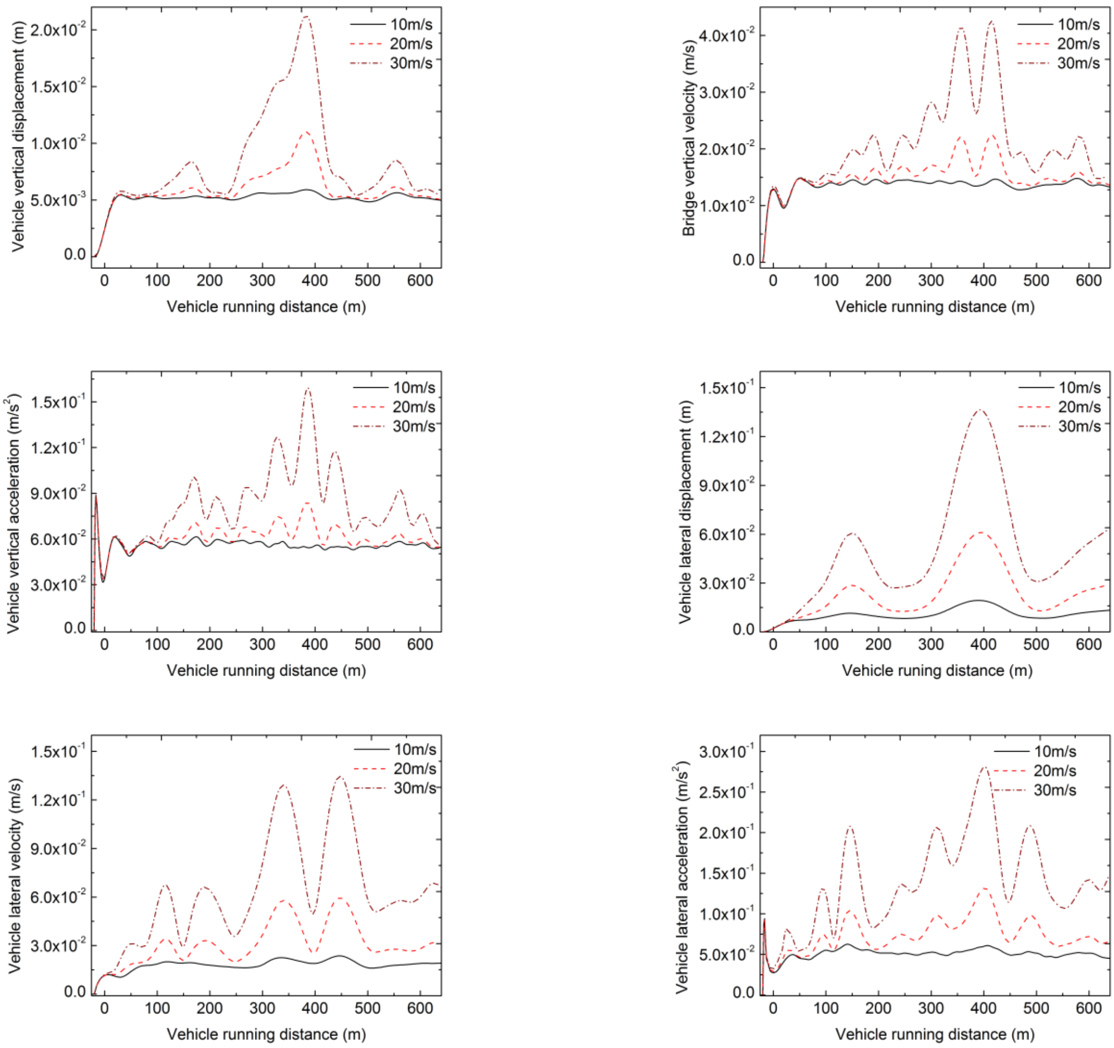

Fig. 16 The standard deviation of vehicle responses with different wind velocity

responses. When running speed is 200 km/h, the lateral acceleration is smaller than the other case and the cumulative probability is stable with the growth of responses. Therefore, the running speed has impact on both the dynamic responses of train andbridge. The running speed has a significant contribution on the maximum of the standard deviation of vehicle responses, but the maximum of the standard deviation of bridge responses is not sensitive to the vehicle speed.

3.5 The effect of wind velocity on the coupling system subjected to wind loads

The wind velocity of 10 m/s, 20 m/s, and 30 m/s are taken into account in the case study to investigate the effect on the vehicle-bridge coupling system, and the other parameters are same as section 3.3. The calculated results are shown in Figs. 16 and 17. The standard deviation of the coupling system is apparently increasing with the rising wind velocity. The vehicle acceleration reaches the maximum when vehicle is running at the middle of main bridge. And when bridge acceleration gets the maximum, the vehicle is just step on the bridge deck. The maximum of coupling system acceleration is shown in Tables 4 and 5.

Table 4 The maximum of vehicle acceleration with different wind velocity (m/s^2)

Wind velocity (m/s)	Vehicle vertical acceleration	Vehicle lateral acceleration
10	0.069	0.063
20	0.084	0.132
30	0.159	0.281

Table 5 The maximum of bridge acceleration with different wind velocity (m/s^2)

Wind velocity (m/s)	Bridge vertical acceleration	Bridge lateral acceleration
10	0.016	0.036
20	0.061	0.096
30	0.136	0.221

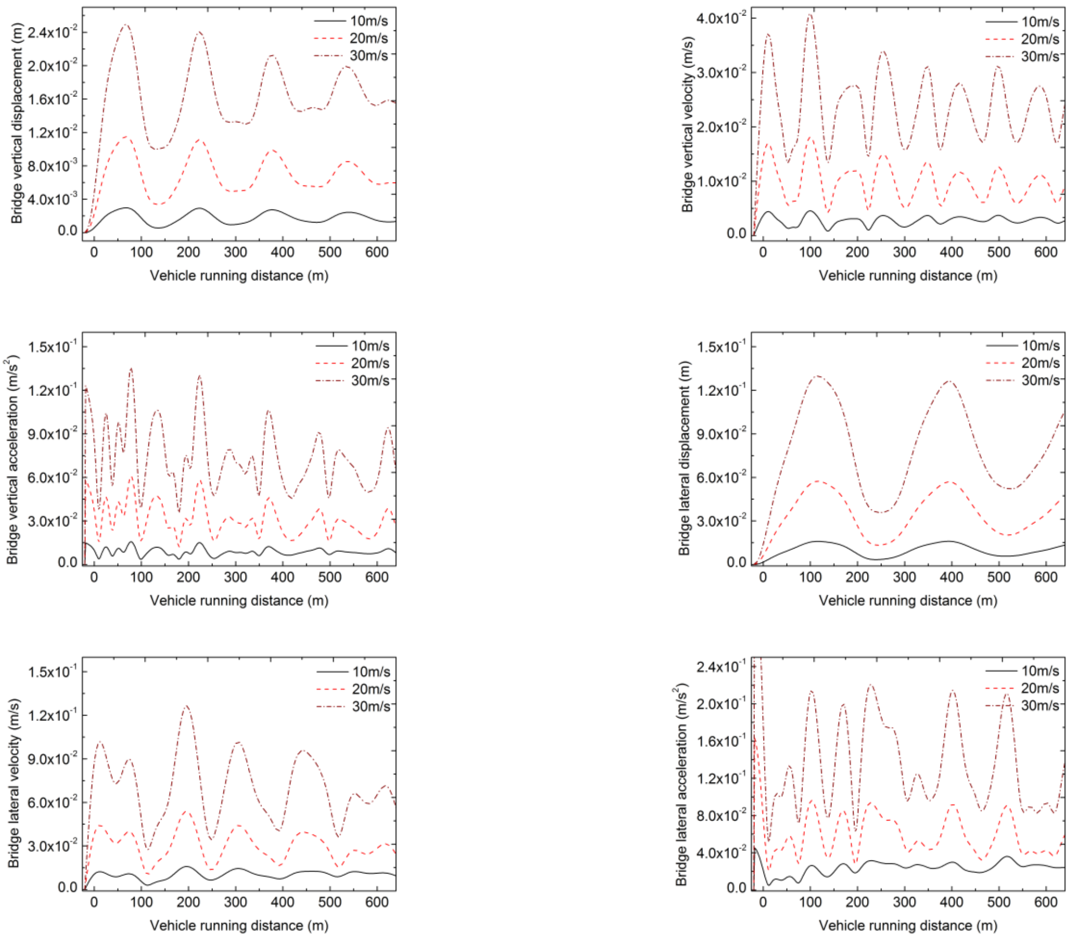

Fig. 17 The standard deviation of bridge responses with different wind velocity

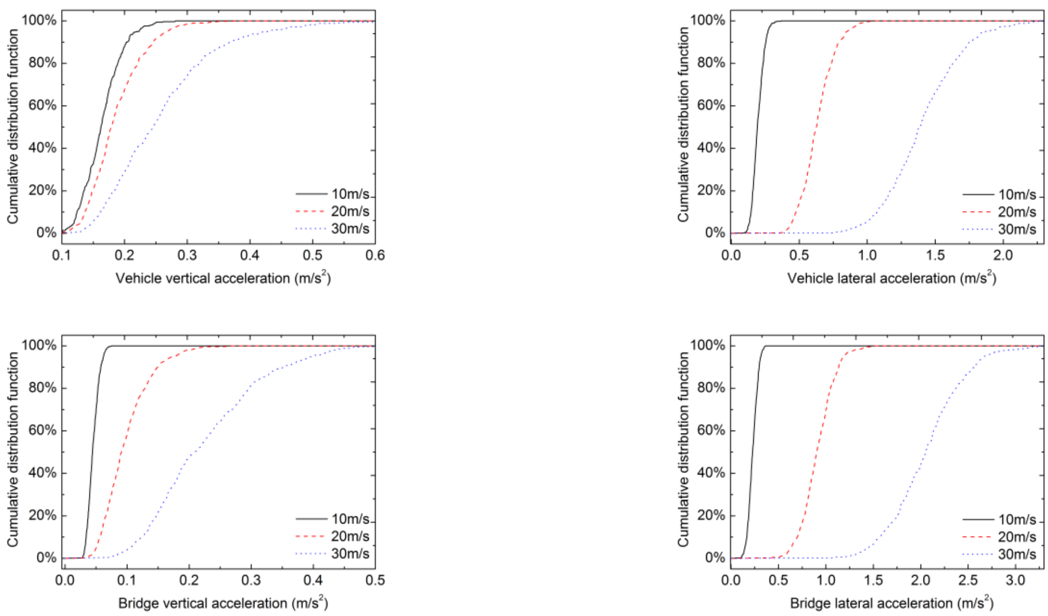

Fig. 18 The CDF of vehicle-bridge coupling system with different wind velocity

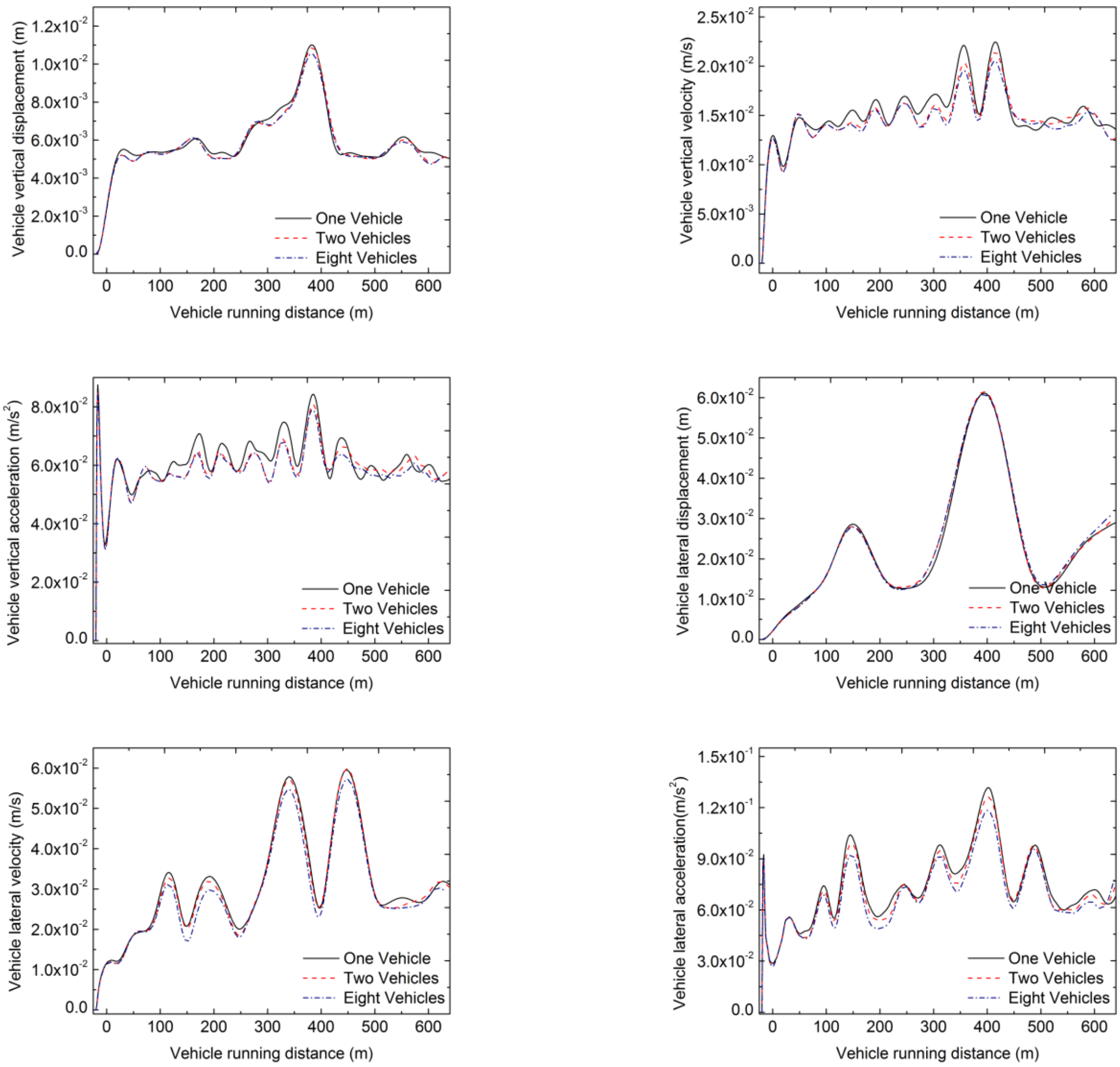

Fig. 19 The standard deviation of vehicle responses with different train marshaling

If wind velocity has doubled, the standard deviation of lateral acceleration and the bridge vertical acceleration would have doubled as well. But the growth of vertical acceleration of vehicle is small. Therefore, vehicle-bridge system is significantly sensitive to the wind velocity, and the effect of wind on the vehicle vertical acceleration is less than that on the other acceleration. The CDF of the coupling system with the different wind velocity is also calculated in Fig 18. With the increasing wind velocity, the range of coupling system responses is rapidly rising. When the same axis is applied in shown results, the curve of lateral acceleration

and the bridge vertical acceleration are almost perpendicular line which means the range of the responses at the low wind velocity compared with that at the high velocity is small enough to be neglected. The randomness and complicacy of coupling system responses at the high wind velocity is much more than that at the low velocity.

3.6 The effect of train marshaling on the coupling system subjected to wind loads

The requirement of passenger and cargo for the railway vehicle is increasing with the social and technological development. The railway vehicle marshaling plays an essential role in dynamic responses of vehicle-bridge coupling system. The effect of train marshaling on the system subjected to wind loads is studied. The calculated results are shown in Figs. 19 and 20. The CDF of the effect of train marshaling on the coupling system is presented in Fig. 21. As the shown in Figs. 19 and 20, the effect of train marshaling on the stochastic responses of coupling system is small for both case. The connections between the marshaling are not considered, which leads to the result that the dynamic responses of one single marshaling could not directly affect the other one. Since the wind loads dominate the standard deviation of bridge responses and the effect of vehicle loads is relatively small, the stochastic vibration of

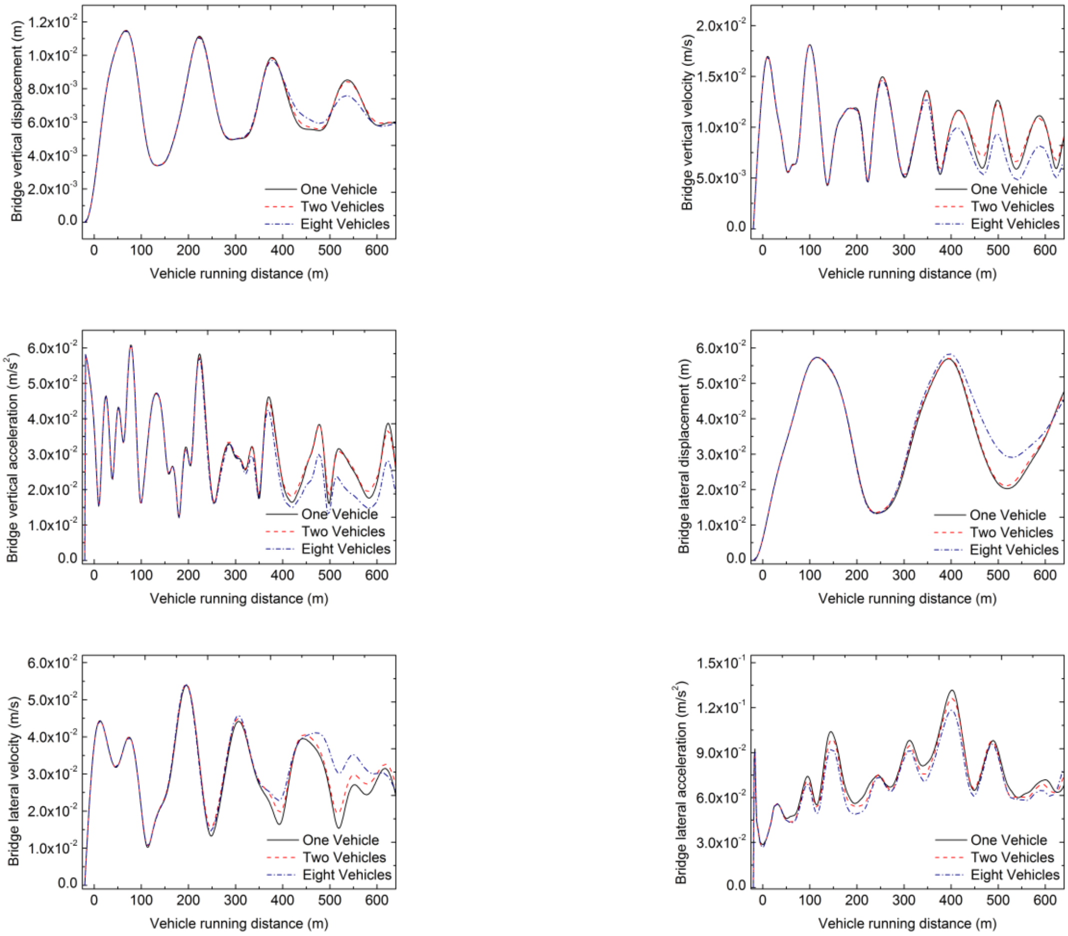

Fig. 20 The standard deviation of bridge responses with different train marshaling

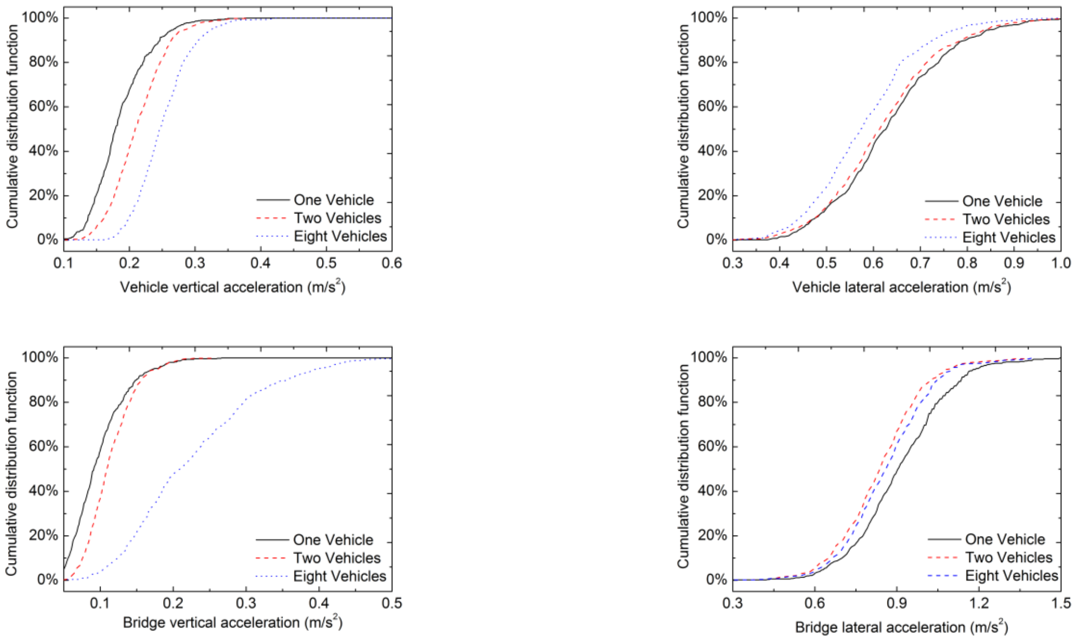

Fig. 21 The CDF of vehicle-bridge coupling system with different train marshaling

bridge, which is feedback to the vehicle, is also in the control of wind loads. Therefore, the effect of marshaling of running vehicle on the standard deviation of coupling system is small. However, the effect of train marshaling on the CFD is significant, especially on the CFD of vertical responses of coupling system. This is because that the train marshaling has an essential affect on the mean value of coupling system. The mean value is increasing with the growth of the number of marshaling.

4. Conclusions

The stochastic responses of vehicle-bridge coupling system subjected to wind loads are investigated by Monte Carlo method. The independent relationship between rail irregularities and wind loads is determined. Moreover, the effects of vehicle running speed, wind velocity and train marshaling on coupling system are also presented.

The effect of wind loads is independent of the effect of rail irregularities on the stochastic responses of coupling system. The bridge responses are in control of wind excitations, the effect of rail irregularities on bridge is not significant. The contribution of rail irregularities to vehicle approximately equal to the contribution of the wind loads. It means that, when the influence factor of each excitation is different, just need to calculate the effect of the changed excitation and combine the intrinsic effect to present stochastic responses of coupling system subjected to wind loads. It leads to reduce the cost of computation.

The randomness of vehicle-bridge coupling system becomes stronger with the growth of vehicle running speed. The vertical acceleration of vehicle is increasing with the development of running speed. The other responses of coupling system are also in control of wind excitations.

The stochastic vibration of vehicle-bridge coupling system is rapidly rising with the increasing wind velocity. The range of coupling system responses at the high wind velocity is much bigger than that at the low wind velocity. A more in-depth understanding is required for the randomness and complexity of the responses.

Since the wind excitation is key influence factor to the vehicle-bridge coupling system, the train marshaling has a little effect on the standard deviation of coupling system. But the marshaling could give a great contribution on the mean value of bridge. Therefore, the effect of train marshaling on the CFD is significant, especially on the CFD of vertical responses of coupling system.

Acknowledgments

The authors are grateful for the financial supports from the National Natural Science Foundation of China (No. 51525804), the Sichuan Province Youth Science and Technology Innovation Team (2015TD0004) and the National Key Technology R&D Program (No. 2012BAG05B02).

References

01-2004 J T G T D (2004), Wind-resistant Design Specification for Highway Bridges.

Aua, F.T.K., Wangb, J.J. and Cheung, Y.K. (2002), "Impact study of cable-stayed railway bridges with random rail irregularities", *Eng. Struct*., **24**, 529-541.

Cai, C.S., Hu, J., Chen, S., Han, Y., Zhang, W. and Kong, X. (2015), "A coupled wind-vehicle-bridge system and its applications: A review", *Wind Struct*., **20**(2), 117-142.

Caprani, C.C. (2014), "Application of the pseudo-excitation method to assessment of walking variability on footbridge vibration", *Comput. Struct*., **132**, 43-54.

Cheli, F., Ripamonti, F., Rocchi, D. and Tomasini, G. (2010), "Aerodynamic behaviour investigation of the new EMUV250 train to cross wind", *J. Wind Eng. Ind. Aerod*., **98**, 189-201.

Deodatis, G. (1996), "Simulation of ergodic multivariate stochastic processes", *J. Eng. Mech*., **122**, 778-787.

Duan, Y.F., Xu, Y.L., Fei, Q.G., Wong, K.Y., Chan, K.W.Y., NI, Y.Q. and NG, C.L. (2011), "Advanced finite element model of Tsing Ma Bridge for structural health monitoring", *Int. J. Struct. Stab. Dyn*., **11**, 313-344.

ElGawady, M.A. and Sha'lan, A. (2011), "Seismic behavior of self-centering precast segmental bridge bents", *J. Bridg. Eng*., **16**, 328-339.

Gullers, P., Andersson, L. and Lundén, R. (2008), "High-frequency vertical wheel–rail contact forces—Field measurements and influence of track irregularities", *Wear*, **265**, 1472-1478.

Jiahao, L. (1992), "A fast CQC algorithm of psd matrices for random seismic responses", *Comput. Struct*., **44**, 683-687.

Jones, N.P. and Scanlan, R.H. (2001), "Theory and full-bridge modeling of wind response of cable-supported bridges", *J. Bridg. Eng*., **6**, 365-375.

Kwon, S.D., Lee, J.S., Moon, J.W. and Kim, M.Y. (2008), "Dynamic interaction analysis of urban transit maglev vehicle and guideway suspension bridge subjected to gusty wind", *Eng. Struct*., **30**, 3445-3456.

Li, Q., Xu, Y.L., Wu, D.J. and Chen, Z.W. (2010), "Computer-aided nonlinear vehicle-bridge interaction snalysis", *J. Vib. Control*, **16**, 1791-1816.

Li, Q.C. and Lin, Y.K. (1995), "New stochastic theory for bridge stability in turbulent flow. II", *J. Eng. Mech*., **121**, 102-116.

Lin, J., Zhang, W. and Williams, F.W. (1994), "Pseudo-excitation algorithm for nonstationary random seismic responses", *Eng. Struct*., **16**, 270-276.

Lin, J.H., Zhang, Y.H. and Zhao, Y. (2011), "Pseudo excitation method and some recent developments", *Procedia Eng*., **14**, 2453-2458.

Lin, J.H., Zhang, Y.H., Li, Q.S. and Williams, F.W. (2004), "Seismic spatial effects for long-span bridges, using the pseudo excitation method", *Eng. Struct*., **26**, 1207-1216.

Lin, Y.K. and Li, Q.C. (1993), "New stochastic theory for bridge stability in turbulent flow", *J. Eng. Mech*., **119**, 113-127.

Lombaert, G. and Conte, J.P. (2012), "Random vibration analysis of dynamic vehicle-bridge interaction due to road unevenness", *J. Eng. Mech*., **138**, 816-825.

Lu, F., . Lin, J.H., Kennedy, D. and Williams, F.W. (2009), "An algorithm to study non-stationary random vibrations of vehicle–bridge systems", *Comput. Struct*., **87**, 177-185.

Madshus, C. and Kaynia, A.M. (2000), "High-speed railway lines on soft ground: dynamic behaviour at critical train speed", *J. Sound Vib*., **231**, 689-701.

Majka, M. and Michael, H. (2009), "Dynamic response of bridges to moving trains: A study on effects of random track rregularities and bridge skewness", *Comput. Struct*., **87**, 1233-1252.

Peng, L., Huang, G., Kareem, A. and Li, Y. (2016), "An efficient space-time based simulation approach of wind velocity field with embedded conditional interpolation for unevenly spaced locations", *Probabilist. Eng. Mech*., **43**, 156-168.

Petrini, F. and Bontempi, F. (2011), "Estimation of fatigue life for long span suspension bridge hangers under wind action and train transit", *Struct. Infrastruct. Eng*., **7**, 491-507.

Prenninger, P.H.W., Matsumoto, M., Shiraishi, N., Izumi, C. and Tsukiyama, Y. (1990), "Reliability of bridge structures under wind loading: Consideration of uncertainties of wind load parameters", *J. Wind Eng. Ind. Aerod*., **33**, 385-394.

Raghunathan, R.S., Kim, H.D. and Setoguchi, T. (2002), "Aerodynamics of high-speed railway train", *Prog. Aerosp. Sci*., **38**, 469-514.

Shinozuka, M. (1971), "Simulation of multivariate and multidimensional random processes", *J. Acoust. Soc. Am*., **49**, 357-368.

Wu, Y., Yang, Y. and Yau, J. (2001), "Three-dimensional analysis of train-rail-bridge interaction rroblems", *Veh. Syst. Dyn*., **36**, 1-35.

Xu, Y.L., Ko, J.M. and Yu, Z. (1997), "Modal analysis of tower-cable system of Tsing Ma long suspension bridge", *Eng. Struct.*, **19**, 857-867.

Xu, Y.L., Zhang, N. and Xia, H. (2004), "Vibration of coupled train and cable-stayed bridge systems in cross winds", *Eng. Struct*., **26**, 1389-1406.

Xu, Y.L., Zhang, W.S., Ko, J.M. and Lin, J.H. (1999), "Pseudo-excitation method for vibration analysis of wind-excited structures", *J. Wind Eng. Ind. Aerod*., **83**, 443-454.

Yongle, L., Qiang, S., Liao, H. and Xu, Y.L. (2005), "Dynamics of wind–rail vehicle–bridge systems", *J. Wind Eng. Ind. Aerod*., **93**, 483-507.

Zhang, Z., Zhang, Y., Lin, J., Zhao, Y., Howson, W.P. and Williams, F.W. (2011), "Random vibration of a train traversing a bridge subjected to traveling seismic waves", *Eng. Struct*., **33**, 3546-3558.

Zhang, Z.C., Lin, J.H., Zhang, Y.H., Zhao, Y., Howson, W.P. and Williams, F.W. (2010), "Non-stationary random vibration analysis for train–bridge systems subjected to horizontal earthquakes", *Eng. Struct*., **32**, 3571-3582.

CC